Optimisation of Computer-aided Screen Printing Design

Eszter Horvath, Adam Torok, Peter Ficzere, Istvan Zador, Pal Racz

Department of Electronics Technology, Budapest University of Technology and Economics, Egry József u 18, H-1111 Budapest, Hungary, horvathe@ett.bme.hu;

Department of Transport Technolgy and Economics, Budapest University of Technology and Economics, Sztoczek u. 2, H-1111 Budapest, Hungary, atorok@kgazd.bme.hu;

Department of Vehicle Elements and Vehicle-Structure Analysis; Budapest University of Technology. and Economics; Stoczek u. 2, H-1111 Budapest, Hungary, ficzere@kge.bme.hu;

Kogát Ltd., Eperjes u. 16, H-4400 Nyíregyháza, Hungary, istvan.zador@kogat.hu

Bánki Donát Faculty of Mechanical and Safety Engineering, Óbuda University, Népszínház u. 8, H-1081 Budapest, Hungary, racz.pal@bgk.uni-obuda.hu

Abstract: Computer-aided screen printing is a widely used technology in several fields like the production of textiles, decorative signs and displays and in printed electronics, including circuit board printing and thick film technology. Even though there have been many developments in the technology, it is still being improved. This paper deals with the optimisation of the screen printing process. The layer deposition and the manufacturing process parameters strongly affect the quality of the prints. During this process the paste is printed by a rubber squeegee onto the surface of the substrate through a stainless steel metal screen masked by photolithographic emulsion. The off-contact screen printing method is considered in this paper because it allows better printing quality than the contact one. In our research a Finite Element Model (FEM) was created in ANSYS Multiphysics software to investigate the screen deformation and to reduce the stress in the screen in order to extend its life cycle. An individual deformation measuring setup was designed to validate the FEM model of the screen. By modification of the geometric parameters of the squeegee the maximal and the average stress in the screen can be reduced. Furthermore the tension of the screen is decreasing in its life cycle which results in worse printing quality. The compensation of this reducing tension and the modified shape of squeegee are described in this paper. Using this approach the life cycle of the screen could be extended by decreased mechanical stress and optimised off-contact.

Keywords: screen printing; FEM; optimisation

1   Introduction

Screen printing is the most widespread and common additive layer deposition and patterning method because of its ability to print on many kinds of substrates with the widest range of inks and because, considering any modern print process, it can deposit the greatest thickness of ink film [1]. Although this technology has been used since the beginning of the 2nd millennium it is still under development and there have been many innovations with the technology in the last 50 years [2].

Screen printing technology provides the most cost effective facility for applying and patterning the different layers for hybrid electronics industry as well, since a thick film circuit usually contains printed conductive lines, resistive and dielectric layers. Due to its simple technology and relative cheapness it is still widely used in the mass assembly of recent electronic circuits. The technology has a large application field extending to decal fabrication, balloon and cloths patterning, textile production, producing signs and displays, decorative automobile trim and truck signs and last but not least use in printed electronics [3]. Screen-printing is ideal as a manufacturing approach for microfluidic elements also used in the field of clinical, environmental or industrial analysis [4], in sensors [5] and in solar cells [6].

In general, the layers are designed using computer-assisted design (CAD) software [7]. Paste printing is carried out by a screen printer machine. The screen is strained onto an aluminium frame and the ink is pressed onto the substrate through the screen not covered by emulsion by a printing squeegee. The squeegee has constant speed and pushes the screen with a contact force. The material of the screen can be stainless steel or polymer. The design of the printed layer is realized with a negative emulsion mask on the screens. There are two main techniques of screen printing:

- off-contact, where the screen is warped with a given tension above the substrate;
- contact, where the screen is in full contact with the substrate.

Contact screen-printing is less advantageous in general, because due to the lift off of the screen it often causes the damage of the high resolution pattern.

In case of off-contact screen-printing, some paste is applied on top of the screen in the front of the polymer squeegee. While the squeegee is moving forward, it pushes the screen downwards until it comes into contact with the substrate beneath. The paste is pushed along in front of the squeegee and pushed through the screen not covered by emulsion pattern onto the substrate. The screen and substrate separate behind the squeegee. The off-contact screen printing process is demonstrated in Fig. 1.
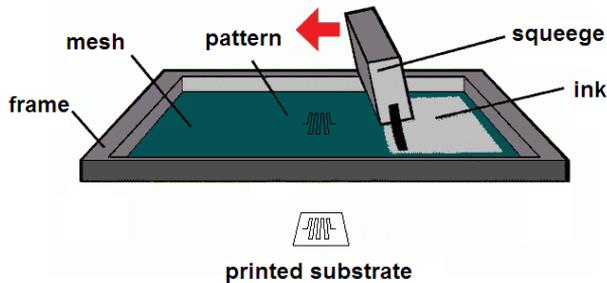
Figure 1
The squeegee pushes the paste on the screen and presses it through the openings

Since the 1960s several experiments and models of the printing process have been evaluated. The optimisation of screen printing was mainly achieved by experimental evaluation without the advantage of numerical models. The empirical optimisation method is described by *Kobs* and *Voigt* [8] in *1970*, they appointed more than 50 variables and combined the most important ones in almost 300 different ways and also compared the effects of them. These investigations offer an enormous empirical database but general rules for screen-printing cannot be created from this without models. Miller [9] has investigated the amount of paste printed on the substrate in the function of paste rheology, mesh size and line width. Others have examined the influence of squeegee angle and squeegee blade characteristic on the thickness of the deposited paste [10] and the effect of the screen on fine scale printed patterns [11]. In general, the best solution for optimising a process can be achieved by parameter optimisation based on a theoretical model [12].

The first efforts to achieve a theoretical description of the screen printing process were made by *Riemer* more than 20 years ago [13-15]. His mathematical models of the screen-printing process were based fundamentally on the Newtonian viscous fluid scraping model [16]. This model was extended by others [17-18], although they did not take into account the flexibility of the screen, which is a feature influencing the process essentially. Neither of these models deals with the effect of geometry in the screen printing process. The repetitive behaviour of the printing process requires taking into consideration the effect of the cyclic load. In this work, a mechanical model is presented with similar geometry to the off-contact screen printing process. In this model, instead of the paste deposition phase, the mechanical behaviour of the screen is in the focus. Furthermore, our model effectively considers the geometry of the knife. The aim of this paper is to improve the technical solutions and in increase the performances without harming reliability as defined at Morariu [26].

2   Experimental Setup

2.1   Material Parameters of Screen

The first step of the model construction is to define the geometries and obtain the mechanical parameters of the screen [27]. The geometric features and the initial strain – which warps it onto an aluminium frame – are realised by the manufacturing process.

In order to decrease screen tension deviation during the print the screen is tightened onto the aluminium frame with the thread orientation of 45° to the printing direction. Therefore the load distribution is more homogeneous between the threads.

The elastic (Young) modulus of the screen was determined using the modified Voigt expression:

$$E_c = \eta \cdot E_f \cdot V_f + E_m \cdot (1 - V_f) \tag{1}$$

where
E_m = 690 MPa is the elastic modulus of the emulsion,
E_f = 193 GPa is the elastic modulus of the stainless steel,
V_f is the volume fraction of the stainless steel and
η is the Krenchel efficiency factor [19], [20].

In case of $\Theta_1 = \Theta_2 = 45°$ thread orientation in the frame:

$$\eta = 0.5 \cdot \cos^4 \Theta_1 + 0.5 \cdot \cos^4 \Theta_2 = 0.25 \tag{2}$$

The Poisson ratio can be expressed as:

$$\nu_{xy} = \nu_f \cdot V_f + \nu_m \cdot V_m \tag{3}$$

where
ν_f is the Poisson´s ratio of stainless steel (0.28) and
ν_m is the Poisson ratio of emulsion (0.43) [21].

In our study SD75/36 stainless steel screen was utilised with the mesh number of 230 and open area of 46%. The schematic view of screen cross section is shown in Fig. 2,
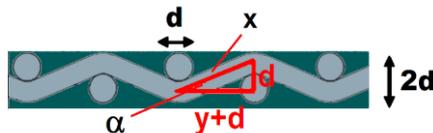

Figure 2
A sketch of the SD75/36 screen cross section with the main parameters

where

d is the diameter of the thread,

α is the bending angle,

x is the element length of the thread.

$$x = \frac{d}{sin\,\alpha}$$

(4)

Using Eq.4. the volume fraction of the stainless steel can be calculated:

$$V_f = 2 \cdot \frac{d^2 \cdot \pi}{4} \cdot l \cdot \frac{l}{l+d} \cdot \frac{d}{sin\,\alpha} = 0.27$$

(5)

Substituting Eq. 5. into Eq. 1. the elastic modulus of the screen turned out to be 13 GPa. The sizes of the screen are 298 mm in width, 328 mm in length and the thickness of it was 72 μm. These parameters were utilised in the finite element model.

2.2 Measuring the Friction Force between the Screen and the Squeegee

The paste we have applied in our experiment was PC 3000 conductive adhesive paste from Heraeus. In the process of screen printing the friction force between the screen and the squeegee plays an important role. While the squeegee passes the screen due to the friction force the position of the mask shifts. The individual friction force measuring setup is shown in Fig. 3.
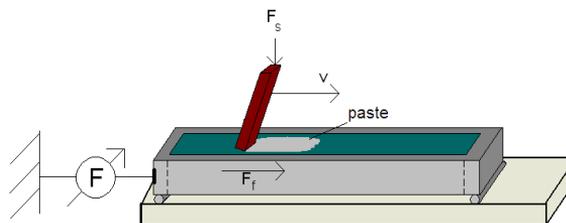

Figure 3

Measurement setup for determining the friction force between the squeegee

By this measurement the relationship between the friction force (F_f) and the printing speed (v) and squeegee force (F_s) was estimated. Every thick film paste is viscous and has a non-Newtonian rheology suitable for screen printing. The shear stress, τ, for this kind of fluids can be described by the Ostwald de Waele relationship:

$$\tau = K\left(\frac{dv}{dy}\right)^n \tag{6}$$

where

K is the flow consistency coefficient (Pa·s^n),

$\partial v / \partial y$ is the shear rate or the velocity gradient perpendicular to the plane of shear (s^{-1}),

n is the flow behaviour index (-) [22].

Fig. 4 shows the shear stress and paste velocity during screen printing. Thick film paste is a shear-thinning fluid, thus n is positive but lower than 1.
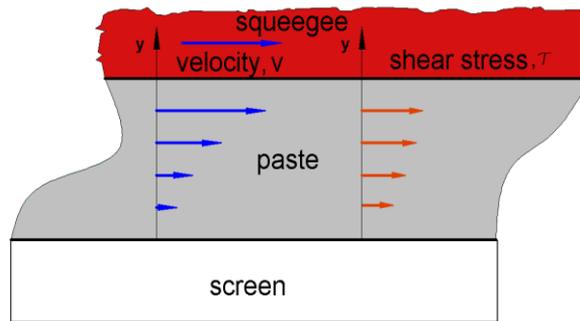

Figure 4

Appeared shear stress and the velocity of paste during screen printing.

In addition the elongation of the screen – which is greater if the off-contact is greater – results in image shift as well [23]. The effect of these lateral shifts demonstrated in Fig. 5 has also to be taken into account.
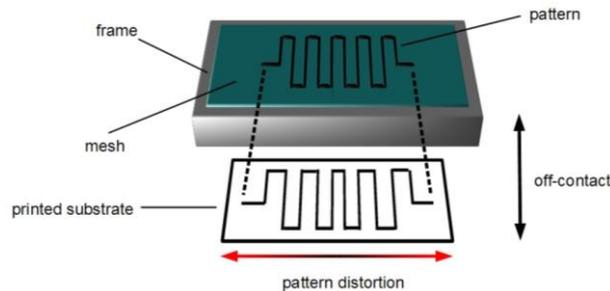

Figure 5

Deformed paste deposition is the result of the screen elongation

The image shift was examined, where the screen tension was in the region of 2–3.3 N/mm, the off-contact was 0.9–1.5 mm, and the applied friction force was based on the measurement. The reduction of screen tension can affect the quality of the printing in other respects. The deflection force of the screen is decreasing,

so the separation of the substrate and the screen cannot start right after the squeegee passes on the screen. This off-contact distance has to be modified in the function of screen tension to keep the screen from sticking to the substrate during printing because adhesion causes many separation problems that damage the quality of the printed film.

2.3   Principles of the Mechanical Model

Equations for mechanical simulations are based on the stress strain relationship for linear material [24]:

$$\sigma_{ij} = C_{ijkl}\varepsilon_{kl} \tag{7}$$

   where
   σ is the stress tensor,
   C is fourth order elasticity tensor and
   ε is the elastic strain tensor.

The stiffness matrix can be reduced to a simpler form because the material is symmetric in the x and y direction. The elastic stiffness matrix has the following form:

$$D = \frac{E}{(1+v)\cdot(1-2v)} \begin{bmatrix} 1-v & \iota & 0 \\ v & 1-v & 0 \\ 0 & 0 & \frac{1-2v}{2} \end{bmatrix} \tag{8}$$

   where
   E is the Young modulus,
   v is Poisson ratio.

As a consequence of the squeegee load the screen bends and gets large displacement or so called geometric nonlinearity. The resulting strains are calculated by using Green-Lagrange strains, where that is defined with reference to the undeformed geometry. Green-Lagrangian strain components, E_{ij}, can be expressed as:

$$E_{ij} = \frac{1}{2}\left(\frac{\partial u_i}{\partial x_j} + \frac{\partial u_j}{\partial x_i} + \frac{\partial u_k}{\partial x_i} \cdot \frac{\partial u_k}{\partial x_j} \right) \tag{9}$$

where $\boldsymbol{u}$ is the displacements vector.

2.4   Constructing and Verifying the Finite Element Model

For the screen model SHELL 93 element was selected because it handles nonlinear geometry in large strain/deflection and in stress stiffening. These two types of geometric nonlinearities are playing significant role in modelling the mechanical description of the screen. SHELL93 element has six DOF (degrees of freedom) at every node. The first step in modelling the screen was to determine the initial strain in the screen without additional load, due to the fact that it tightens on the frame. These loads were applied on two perpendicular edges of the screen, while the two others were fixed in the direction of the load acting at the opposite edge. The schematic view of the sizes (*x*=328 mm, *y*=298 mm), edge loads (σ_x, σ_y) and constraints can be seen on Fig. 6.
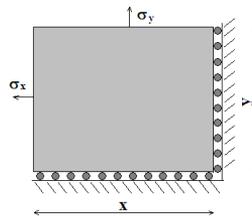
Figure 6

Layout of the pre-stress condition

In the second model – in which the bending of the screen is calculated in the function of load value and position – the screen tightness is given by a displacement constraint calculated in the model before. As boundary conditions, fixed screen edges (in all direction the displacements and rotations are zero) with the calculated displacement conditions were given. Taking into consideration that the printing process is slow enough, it can be handled stationary in each moment while the screen is in force equilibrium. The width of the squeegee was 180 mm. Rectangular elements were used and the mesh density was gradually increasing only towards the load area of the squeegee for faster convergence. The aim of this simulation was to examine how the model describes the real process. In order to compare the FEM calculation to the real situation a measurement set-up was designed and realised (Fig. 7).
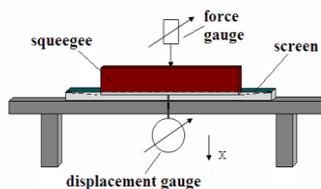

Figure 7

A sketch of the equipment for measuring deformation of the screen

The screen was loaded at 11 different positions, where the distances from the centre range from 0 mm to 100 mm with 10 mm step sizes, represented in Fig. 8. The load was 40-80 N in 10 N step sizes. These parameters give 55 different measurement points. At one measurement point five measurements were recorded.
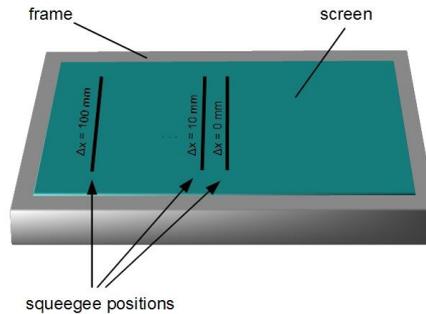

Figure 8
The squeegee line locations on the screen during the measurement

In the model of screen-printing, the displacement of the screen at the load place in direction z was maximised according to the industrial standards of distance (about 1 mm) between the screen and the substrate (off-contact) [25]. The original construction of the screen printing is shown in Fig. 9.
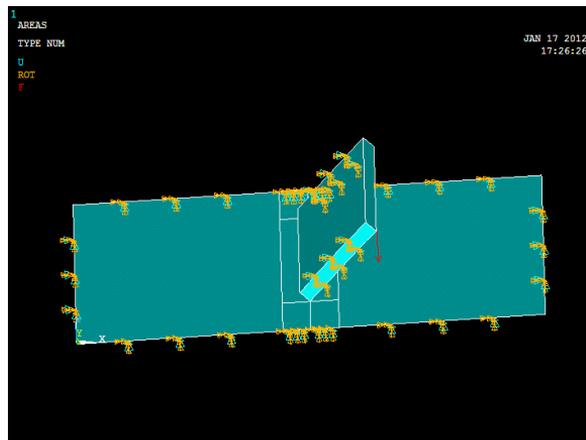

Figure 9
The original construction of screen printing in FEM model with the constraints

As boundary conditions, fixed screen edges (motion is zero in all possible direction) were set with the displacement load in x and y direction which corresponds to the screen tension. A finer mesh was created in that area where the squeegee acts and a coarser mesh for the rest of the model (Fig. 10).
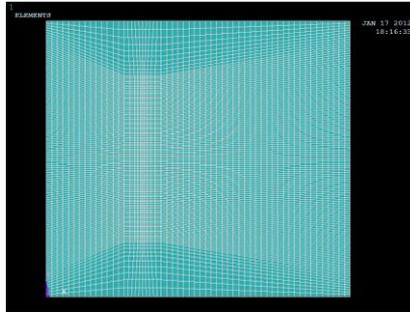
Figure 10

Meshed screen in FEM; the mesh is densified at the load area of the squeegee.

The finer-meshed area ensures accuracy the coarser-meshed area provides faster run time.

3   Results and Discussion

3.1   Modelling of Stress Distribution in the Screen

In the first model of the screen the initial strain – caused by the stretching on the frame – was determined. For the initial stress of $\sigma_x = \sigma_y = 2.65$ N/mm the displacements in direction *x* and *y* were -0.6209 mm and 0.5641 mm respectively. In the second model the screen tightness is given by this displacement constraint calculated in the model before. In this model the screen was loaded at 11 different positions and five different loads were applied according to the measurements. Compared to the simulation results and measurements the screen deformation can be seen in Fig. 11 for 55 different conditions.
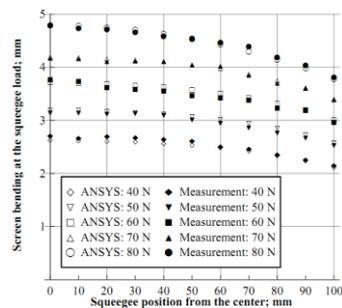

Figure 11

Measured and simulated bending of the screen at load line

In the model of screen printing – where the maximal displacement of the screen in direction z was 1 mm – the stress was concentrated at the ends of the load area (Fig. 12).
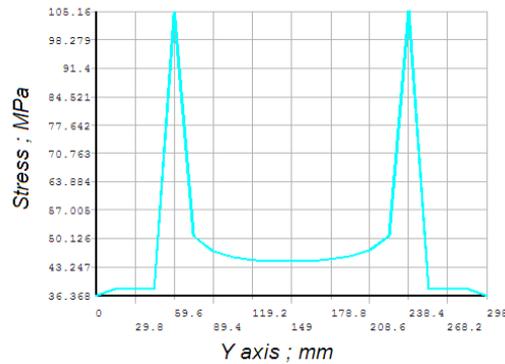

Figure 12

Von Mises equivalent stress distribution in the screen along the line, where the load is applied

The maximal stress in the screen (105 MPa) appeared around the load edge while the average stress in the screen was only about 38 MPa. This phenomenon occurred due to the squeegee shape ending in a point so the corners of the squeegee generate stress concentration in the screen. The surface quality of a used screen (5000 cycles) was examined by optical microscope to detect the damage caused by these high stress peaks (Fig. 13). Investigation shows that the screen area, where the edges of the squeegee passed the filaments are abraded, while the middle part is intact.
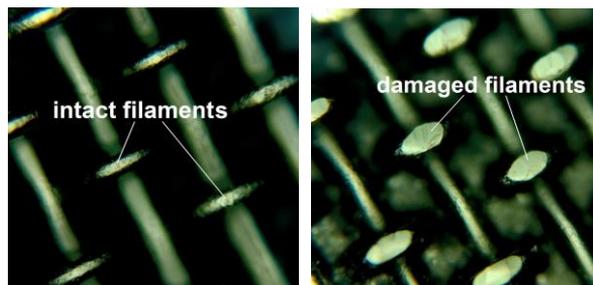

Figure 13

The middle part of the screen is intact but where the squeegee edges act the filaments are abraded

In order to reduce this relative high stress peak in the material the shape of the squeegee was modified (Fig. 14). The two parameters of the rounding are R and f, the radius of the circle and the width of the rounded squeegee segment respectively.
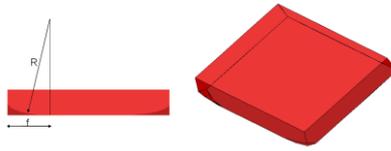
Figure 14

Squeegee rounding scheme with the radius of the circle and the width of the rounded squeegee
segment

The optimal radius can be obtained from the extrema (in this case the minimum)
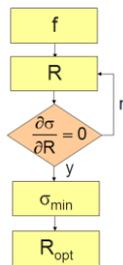of the $\sigma(R)$ stress-radius function (Fig. 15).

Figure 15

Process flow of the squeegee – rounding optimisation

As the result of the rounded squeegee, in case of $f = 40$ mm with the optimal R of
1900 mm, the maximal stress in the screen reduces to half (Fig. 16).
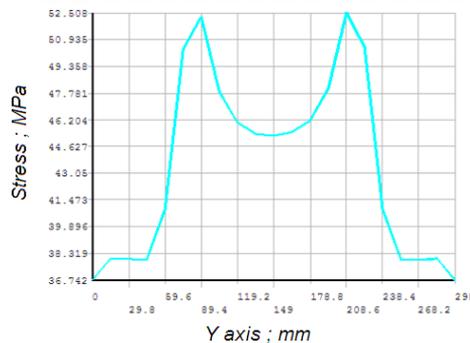

Figure 16

Von Mises equivalent stress distribution in the screen along the line, where the load is applied

The value of f should be as high as the screen mask allows, because larger
rounded area results in lower stress concentration. During screen printing the
geometry of the squeegee, so the shape of the curvature can be changed.

Therefore, further simulation was carried out to determine the deformation of the squeegee for different loads. Fig. 17 shows the deformation of the squeegee in direction Z (vertical axis that perpendicular to basic surface):
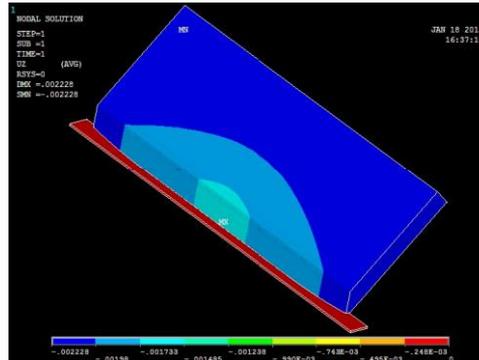

Figure 17

Displacement of the squeegee in direction Z in case of the load of 50 N

The result of the simulation shows that the maximal deformation of the squeegee is equal to the squeegee shape with a cutting process accuracy of +/- 0.02 mm so this can be neglected in the final model.

3.2   Effect of the Friction Force and Screen Tension in the Quality of Screen Printing

The model was supplemented by the friction force (see Section 2.2) in order to determine the shift of the patterned screen. *Table 1* summarises the friction force between the screen and the squeegee as a function of the squeegee force and speed.

Table 1

The friction force between the screen and the squeegee*

Speed [mm/s] / Squeegee pressure [N]	20	40	60	80	100	120	140	160
10	2.2	3.4	4	4.6	4.6	5.2	5.6	5.6
20	2.6	4	4.4	5.2	5.4	5.6	6	6.2
30	3.4	4	4.6	5.2	5.6	5.8	6.8	6.6
40	3.6	4.2	5	5.4	5.8	6	6.8	7
50	3.6	4.6	5	5.4	5.8	6.2	7	7
60	3.8	4.6	5.2	6	5.8	6.4	7.2	7.4
70	4.6	5	5.6	6.2	6.2	6.6	7.4	8
80	4.8	5.6	5.8	6.6	6.6	6.9	8.4	8.4

* at different squeegee force and speed

Evaluating the results of *Table 1* it can be determined by regression of least squares method, that *n* is between 0.2 and 0.4 in Eq. 6 for this type of adhesive paste. Even if the applied friction force was 8.4 N, the off-contact was 1.5 mm and the tension of the screen is reduced to only 2 N/mm the resulted shift is less than 2.7 μm. The image deformation arising from the elongation of the screen is less than 0.5 μm in the printing area of the screen in case of 1.5 mm off-contact. Obviously it is lower if the off-contact is lower. Accordingly the deposition shift is negligible under 1.5 mm off-contact and if the friction force is in this region. However, if there is not enough paste on the screen the friction force can be multiplied, so the shift can reach 10 μm. On the other hand the quality of the printing is maintainable if the reduction of screen tension is compensated. The screen tension is reducing in the screen caused by repetitive printing – which can be handled as a cyclic mechanical load – when the elongation of the screen is increasing. As the tension is decreasing the deflection force of the screen is also decreasing, so the screen usually adheres to the substrate and the separation cannot start right after when the squeegee has passed on the screen. The deflection force is maintainable if the off-contact distance is modified. In our study the initial screen tension was 3 N/mm and the off-contact was the industrial standard (1 mm) which resulted in adequate printing quality. In order to avoid adhering, the off-contact has to be increased according to Fig. 18.
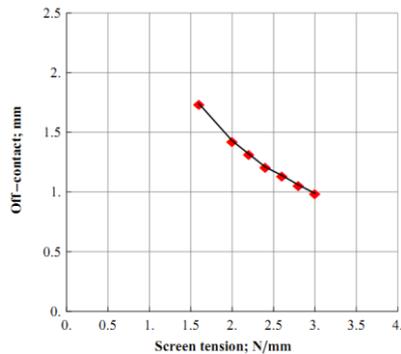

Figure 18

Off-contact compensation in the function of screen tension

As the squeegee force has not been changed, the paste is being printed with the same pressure, and due to the modified off-contact the elastic force resulting from screen deflection and the paste adhesion has the same force condition as at the initial screen tension and off-contact.

Conclusion

A finite element model was created and verified to describe the stress distribution in the screen due to squeegee load. The boundary displacement condition was determined in the first step by the preliminary model. Using these results a model was constituted to simulate the bend of the screen due to different loads acting at

different positions. A measurement set-up was designed and realised to verify the model. Comparing the measured and simulated results it can be clearly concluded that the model gives good approximation of the bending values. In the model of screen printing – where the maximal displacement of the screen in direction z was 1 mm – the stress was determined. The maximums appeared at the ends of the load area. The geometric parameters of the squeegee were modified to reduce the stress in the screen in order to extend its life cycle. By this the maximal and average stress in the screen could be reduced. Furthermore the decreasing screen tension was compensated by modifying the value of the off-contact which leads to sustainable screen-printing quality. Therefore the life cycle of the screen could be extended by decreased mechanical stress and increased off-contact.

Acknowledgement

References

[1]   Anderson J., Forecasting the Future of Screen-Printing Technology, *Screen Printing Magazine*, October, 2003

[2]   Kosloff A., Photographic Screen Printing, *ST Publications*, Cincinnati, Ohio, 1987

[3]   Selejdak J., Stasiak-Betlejewska R., Determinants of Quality of Printing on Foil, *Journal of Machine Engineering*, Vol. 7, No. 2, 2007, pp. 111-117

[4]   Albareda-Sirvent, M., A. Merkoçi, and S. Alegret, Configurations used in the Design of Screen-printed Enzymatic Biosensors. A review. *Sensors and Actuators B: Chemical*, 2000, 69(1-2) pp. 153-163

[5]   Viricelle J. P., Compatibility of Screen-Printing Technology with Microhotplate for Gas Sensor and Solid Oxide Micro Fuel Cell Development. *Sensors and Actuators B: Chemical*, 2006, 118(1-2) pp. 263-268

[6]   Krebs F. C., Large Area Plastic Solar Cell Modules. *Materials Science and Engineering: B*, 2007, 138(2), pp. 106-111

[7]   Núria Ibáñez-García, Julián Alonso, Cynthia S. Martínez-Cisneros, Francisco Valdés, Green-Tape Ceramics. New Technological Approach for Integrating Electronics and Fluidics in Microsystems, *Trends in Analytical Chemistry*, Volume 27, Issue 1, January 2008, pp. 24-33

[8]   D. R. Kobs and D. R. Voigt, Parametric Dependencies in Thick Film Screening. *Proc. ISHM* 18, 1970, pp. 1-10

[9]   Miller L. F., Paste Transfer in the Screening Process, *Solid State Technology*, 1969, pp. 46-52

[10]   Benson M. Austin, Thick-Film Screen Printing, *Solid State Technology*, 1969, pp. 53-58

[11]   Bacher J. Rudolph, High Resolution Thick Film Printing, *Proceedings of the International Symposium on Microelectronics*, 1986, pp. 576-581

[12]   Dyakov I., Prentkovskis O., Optimization Problems in Designing Automobiles, *Transport*, Vol. 23(4), 2008, pp. 316-322

[13]   Riemer E. Dietrich, Analytical Model of the Screen Printing Process: Part 2. *Solid State Technology* 9, 1988, pp. 85-90

[14]   Riemer E. Dietrich. Analytical Model of the Screen Printing Process: Part 1. *Solid State Technology* 8, 1988, pp. 107-111

[15]   Riemer E. Dietrich, The Theoretical Fundamentals of the Screen Printing Process. *Hybrid Circuits* 18, 1989, pp. 8-17

[16]   Taylor G. I., On Scraping Viscous fluid from a Plane Surface. *Miszallangen Angewandten Mechanik*, 1962, pp. 313-315

[17]   Riedler J., Viscous flow in Corner Regions with a Moving Wall and Leakage of fluid. *Acta Mechanica* 48, 1983, pp. 95-102

[18]   Jeong J., Kim M., Slow Viscous Flow Due to Sliding of a Semi-Infinite Plate over a Plane, *Journal of Physics Society*, 54, 1985, pp. 1789-1799

[19]   Cox H. L., The Elasticity and Strength of Paper and Other Fibrous Materials, *British Journal of Applied Physics*, 3, 1952, pp. 72-79

[20]   Krenchel H., Fibre Reinforcement, *Akademisk Forlag*, 1964, Copenhagen, Denmark

[21]   Irgens F., *Continuum Mechanics*, Springer, 2008

[22]   Blair Scott G. W., Hening, J. C., Wagstaff A.: The Flow of Cream through Narrow Glass Tubes, *Journal of Physical Chemistry* (1939) 43 (7) 853-864

[23]   Hohl Dawn: Controlling Off-Contact", 1997, *Specialty Graphic Imaging Association Journal*, Vol. 4, pp. 5-11

[24]   K-J Bathe, *Finite Element Procedures*, Prentice Hall, 1996

[25]   G. S. White, C. J. W. Breward, P. D. Howell, A Model for the Screen-Printing of Newtonian Fluids, *Journal of Engineering Mathematics*, 2006, 54, pp. 49-70

[26]   C. O. Morariu et al.: A New Method for Determining the Reliability Testing Period Using Weibull Distribution, *Acta Polytechnica Hungarica,* 2013, 10/7, pp. 171-186

[27]   János Kundrák, Zoltán Pálmai: Application of General Tool-life Function under Changing Cutting Conditions, *Acta Polytechnica Hungarica,* 2014, 11/2, pp. 61-76